Attosecond Photoelectron Spectroscopy of Metal Surfaces

C.-H. Zhang and U. Thumm

Department of Physics, Kansas State University, Manhattan, Kansas 66506, USA

(Received 7 November 2008; published 25 March 2009)

Recent attosecond-streaking spectroscopy experiments [A. L. Cavalieri *et al.*, Nature (London) **449**, 1029 (2007)] using copropagating extreme ultraviolet (XUV) and infrared (IR) pulses of variable relative delay have measured a delay of approximately 100 attoseconds between photoelectrons emitted by a single XUV photon from localized core states and delocalized conduction-band states of a tungsten surface. We analyze the underlying XUV-photoemission–IR-streaking mechanism by combining a perturbative description of the XUV-photoemission process and the subsequent nonperturbative IR streaking of the photoelectrons. Our calculated time-resolved photoelectron spectra agree with the experiments of Cavalieri *et al.* and demonstrate that the observed temporal shift is caused by the interference of core-level photoelectrons that originate in different layers of the solid.

DOI: 10.1103/PhysRevLett.102.123601 PACS numbers: 42.50.Hz, 42.65.Re, 79.60.-i

During the past few years, advances in ultrafast laser technology [1–7] have enabled the resolution at a time scale of the order of 100 attoseconds (1 as $= 10^{-18}$ s) of the laser-induced electronic dynamics in atoms [8–11] and molecules [12–14]. The recent successful extension of laser-assisted attosecond photoelectron (PE) spectroscopy to solid surfaces [15] promises the time-resolved observation of electronic processes in condensed matter systems that may involve a single active electron [15,16], the correlated dynamics of two electrons [8,17], or collective electronic excitations (plasmons) [18–20]. Thus, as-streaking spectroscopy now provides an ingenious tool for the time-resolved investigation of photoemission from solids that, in addition to such studies on isolated atoms in the gas phase, promises to yield information on (i) the structure and dynamics of delocalized valence and conduction-band states, (ii) electron transport properties in solids, and (iii) the decay of collective excitations near solid surfaces of novel plasmonic devices [19,21].

The basic setup of an attosecond time-resolved photoelectron streaking experiment on a metal surface is illustrated in Fig. 1. An attosecond extreme XUV light pulse is used to release electrons from either bound core levels or delocalized conduction-band (CB) states. The released PEs get exposed to (''streaked by'') the same IR probe pulse that was also used to generate the XUV pulse via harmonic generation [22]. The two laser pulses are thus synchronized with a precisely adjustable time delay τ, and the measured asymptotic PE kinetic energy E depends on τ. By varying τ, a tomographic image of the time-resolved PE kinetic energy distribution $P(E, \tau)$ can be recorded. This method was first successfully applied to isolated atoms in the gas phase [1,9] and, very recently, to tungsten [15] and platinum [17] surfaces. By using attosecond-streaking spectroscopy, Cavalieri *et al.* [15] measured a relative delay of 110 ± 70 as between the detection of PEs that are emitted by absorption of a single XUV photon from $4f$-core and CB levels. Because of their different initial energies, PEs from core and CB levels can be easily separated in the energy-differential spectra. While Cavalieri *et al.* explained their result in terms of a heuristic model that is based on different release depths and escape paths for core and CB electrons, the question remains to what extent a more rigorous quantum-mechanical model can explain the mechanism behind the observed relative delay in the PE spectra.

In this Letter, we apply a quantum-mechanical model in which the XUV-photoemission step is treated in first-order perturbation theory, while the IR streaking of the PEs is included in a nonperturbative way. A quantum-mechanical model for the comparison of laser-assisted photoemission

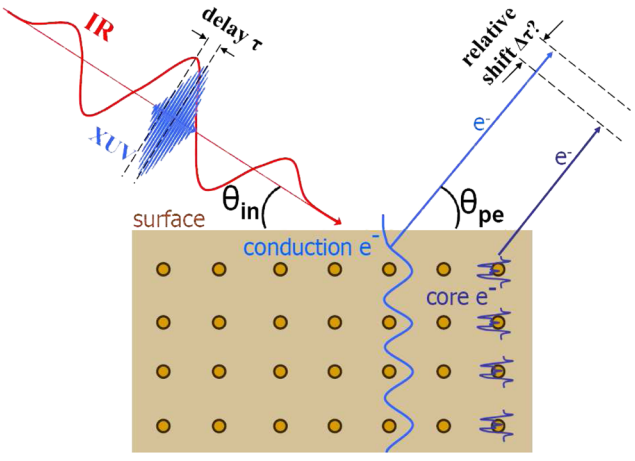

FIG. 1 (color online). Schematic for attosecond-streaking spectroscopy at metal surfaces. Delocalized CB electrons and localized core-level electrons are released by an attosecond XUV pulse (photoelectric effect) and streaked by an IR laser pulse. By changing the delay between the two pulses, the delay between the detection of PEs that originate in CB and core levels can be measured.

from CB and image states of metal surfaces was recently presented by Baggesen and Madsen [16], who used image states as reference states for photoemission from the CB. Their numerical results, however, did not indicate a delay between electron emission from the surface-localized image and delocalized CB states.

To facilitate the comparison with the experiment, we use experimental parameters [15] and model the IR and XUV pulses with Gaussian envelopes $E_{L(X)}(t) \sim e^{-2\ln 2(t/\tau_{L(X)})^2}\cos(\omega_{L(X)}t)$, with pulse lengths $\tau_L = 6.5$ fs and $\tau_X = 0.29$ fs (FWHM) and energies $\hbar\omega_L = 1.7$ eV and $\hbar\omega_X = 91$ eV. The IR peak intensity is $I_L = 2 \times 10^{12}$ W/cm^2. For the W(110) surface, we use measured values for the work function ($W = 5.5$ eV), Fermi energy ($\varepsilon_F = 4.5$ eV), and the lattice constant in the direction perpendicular to the surface ($a = 3.13$ Å). We calculated energy-resolved spectra $P_{\mathrm{CB}}(E, \tau)$ and $P_{4f}(E, \tau)$ for the two groups of PEs as a function of τ. The comparison of experiment and theory in Fig. 2 shows that our IR pulse modulation of the PE kinetic energy agrees with the experiment. In order to find the temporal shift between the two calculated spectra in the right column of Fig. 2, we calculated their center-of-energies (COE) $\bar{E}(\tau)$ [23]. The temporal shift $\Delta\tau$ between $4f$ core-level and CB electrons is recognizable in Fig. 3 for both experimental data and calculation. We found that the measured value of $\Delta\tau = 110$ as can be obtained by adjusting the electron mean free path to $\lambda = 5$ Å, in close agreement with the value for 55 eV electrons on the universal curve for λ [24]. As we show below, $\Delta\tau$ is a result of (i) interference effects between electrons that are photoemitted from $4f$-core levels from different layers in the solid and (ii) a finite mean free path of the PEs inside the solid.

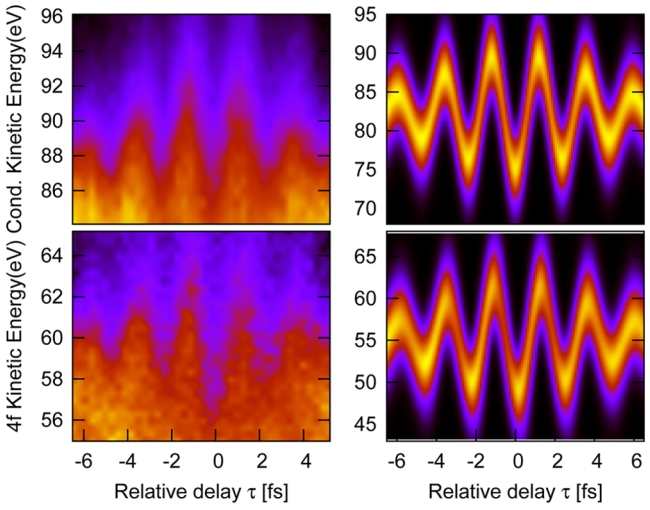

FIG. 2 (color online). Time-resolved PE spectra for emission out of the CB (top) and $4f$-core level (bottom) of a W(110) surface, as a function of the delay between the XUV and IR pulses for decadic color scales. Experimental results of Fig. 3(a) in Ref. [15] (left) in comparison with our calculation (right).

We model the physical scenario [15] in Fig. 1 for grazing incidence of the XUV and IR pulses ($\theta_{\mathrm{in}} = 0$) and photoemission along the surface normal ($z > 0$ direction, $\theta_{\mathrm{pe}} = \pi/2$) because the temporal behavior of the two groups of PEs does not depend on the specific geometry. We describe the XUV photorelease as a one-step single-electron transition [25] from an initial state $\Psi_{\mathbf{k}_i}(\mathbf{r}, t) = \Psi_{\mathbf{k}_i}(\mathbf{r})e^{-i\varepsilon_i t}$ with initial binding energy ε_i to an IR-field-dressed damped final continuum state, in accord with the observed single XUV photoemission and comparatively low frequency and moderate intensity of the IR pulse. The initial state is composed of (i) incident and reflected Bloch waves $\Psi^-_{\mathbf{k}_i}$ and $\Psi^+_{\mathbf{k}_i}$ that describe the motion of an electron inside the solid towards and away from the surface with crystal momenta $\mathbf{k}^{\pm}_i = (\mathbf{k}_{\parallel}, \pm k_z)$ and (ii) a transmitted part that represents the exponential decay of the initial state's probability density into the vacuum ($z > 0$) whose contribution to the transition probability is negligible. At the considered moderate laser intensities, we neglect interband transitions and intraband perturbations. By numerically solving Helmholtz's equations at the metal-vacuum interface [26], we deduced the skin depth $\delta_L \sim 100$ Å for the IR pulse, which is consistent with Ref. [27] and much larger than $\lambda \sim 5$ Å. We therefore consider the IR field amplitude to be constant up to the depth λ in the solid. Keeping in mind that the XUV photon energy $\hbar\omega_X$ is large compared to the energy of all residual final-state interactions, we neglect all interactions of the outgoing PEs with the substrate (including space-charge effects) and represent the final state as a damped Volkov wave $\Psi^V_{\mathbf{k}_f,\kappa}(\mathbf{r}, t) = \Psi^V_{\mathbf{k}_f}(\mathbf{r}, t)\chi(\kappa, z)$, with the damping factor $\chi(\kappa, z) = e^{\kappa z}$

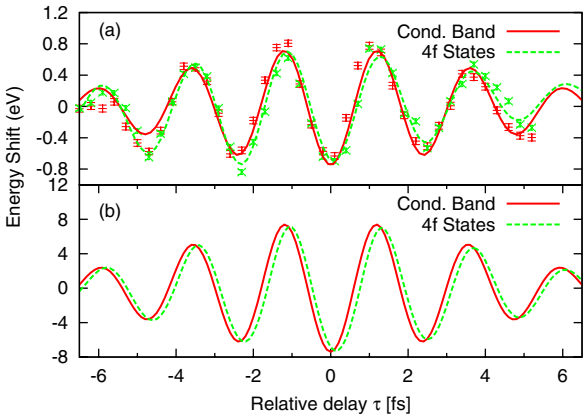

FIG. 3 (color online). Streaked electron spectra for photoemission from CB and $4f$-core levels of a W(110) surface: $\bar{E}$ [23] as a function of the delay between the XUV and IR pulse. (a) Experimental results of Fig. 3(b) in Ref. [15]. The damped sinusoidal curves are fits to the raw experimental data (points with error bars). (b) Calculated results showing a relative shift of $\Delta\tau = 110$ as between the two groups of electrons. For better comparison, COEs for the $4f$ PEs are multiplied by a factor of 2.5 in (a) and 1.1 in (b).

for $z < 0$ and 1 for $z > 0$. $\mathbf{k}_f$ designates the (unstreaked) final momentum of the PE, $\kappa = 1/\lambda$ the damping parameter, and $\Psi^V_{\mathbf{k}_f}$ the usual Volkov wave [28]. We note that a surface-charge layer tends to shift the spectrum as a whole to higher energies [17], with little or no influence on relative temporal shifts.

The PE transition amplitude in the dipole-length gauge for the interaction with the XUV electric field $E_X(t)$ can now be written as

$$T_{\mathbf{k}_f,\mathbf{k}_i}(\tau) = \frac{1}{i}\int_{-\infty}^{+\infty} dt \langle \Psi^V_{\mathbf{k}_f,\kappa}(t)|zE_X(t+\tau)|\Psi_{\mathbf{k}_i}(t)\rangle. \quad (1)$$

We use atomic units throughout this Letter, unless indicated otherwise. The integrand of (1) can be written as $E_X(t)d_{\mathbf{k}_i,\mathbf{p}}(t_d)e^{-i\varepsilon_i t - i\phi_{v,\mathbf{k}_f}(t-\tau)}$, with the Volkov phase $\phi_{v,\mathbf{k}}(t) = \frac{1}{2}\int_t^{+\infty} dt'[\mathbf{k} + \mathbf{A}_L(t')]^2$ and the vector potential for the IR electric field $\mathbf{A}_L(t) = \hat{\mathbf{z}}\int_t^{\infty} dt' E_L(t')$ [29]. $\mathbf{p}(t) = \mathbf{k}_f + \mathbf{A}_L(t)$ is the canonical momentum, $t_d = t - \tau$, and $d_{\mathbf{k}_i,\mathbf{p}}$ is the dipole matrix element (DME). Summation over all $\mathbf{k}_i$ in the first Brillouin zone yields the photoemission probability $P(E,\tau) = \sum_i |T_{\mathbf{k}_f,\mathbf{k}_i}(\tau)|^2$ as a function of the final electron kinetic energy E and τ. Changing the delay τ while recording the final electron kinetic energy distribution allows the attosecond electron dynamics for different initial states to be retrieved from the time-resolved PE spectra.

The temporal shift in the photoemission spectra is contained solely in the DME. Inside the solid, we split the z integral in $d_{\mathbf{k}_i,\mathbf{p}(t)} = (i/\sqrt{V})\frac{d}{dp_z}\int d^3r e^{-i\mathbf{p}\cdot\mathbf{r}} e^{\kappa z}\Psi_{\mathbf{k}_i}(\mathbf{r})$ into the form factor

$$f^{\pm}_{\mathbf{k}_i,\mathbf{p}(t)} = \frac{1}{Sa}\int_S d\mathbf{r}_\parallel \int_{-a}^{0} dz e^{-i\mathbf{p}(t)\cdot\mathbf{r}}\Psi^{\pm}_{\mathbf{k}_i}(\mathbf{r}) \quad (2)$$

and the interlayer structure factor

$$\Delta^{\pm}_{p_z(t),k_z}(\kappa) = \sum_{n=0}^{\infty} e^{i[p_z(t)\pm k_z + i\kappa]na} = \frac{1}{1 - e^{i[p_z(t)\pm k_z + i\kappa]a}}, \quad (3)$$

to obtain

$$d_{\mathbf{k}_i,\mathbf{p}(t_d)} = i\frac{d}{dp_z}\sum_{l=-,+} f^l_{\mathbf{k}_i,\mathbf{p}(t_d)}\Delta^l_{p_z(t_d),k_z}(\kappa), \quad (4)$$

where S is the surface area. In comparison with the case of gaseous targets [28], for a crystalline target the DME includes interfering contributions from different lattice layers in terms of the additional structure factor [25].

In order to proceed, we need to specify the initial state. First, considering photoemission from the CB, we approximate the initial state in the jellium approximation [30] as $\Psi_{\mathbf{k}}(\mathbf{r}) = (1/\sqrt{V})e^{i\mathbf{k}_\parallel\cdot\mathbf{r}_\parallel}(e^{ik_z z} + Re^{-ik_z z})\Theta(-z)$, where $R = (k_z - i\gamma)/(k_z + i\gamma)$ with $\gamma = \sqrt{2(\varepsilon_F + W) - k_z^2}$ and $\Theta(z) = 1$ if $z > 0$ (0 otherwise), and find

$$f^{\pm}_{\mathbf{k}_i,\mathbf{p}(t)} = -\frac{\delta_{\mathbf{p}_\parallel - \mathbf{k}_\parallel} R^{(1/2)\pm(1/2)}}{i[p_z(t) \pm k_z + i\kappa]\Delta^{\pm}_{p_z(t),k_z}(\kappa)}. \quad (5)$$

This results in the DME

$$d^{\mathrm{CB}}_{\mathbf{k}_i,\mathbf{p}(t)} = \frac{1}{a}\left[\frac{\delta_{\mathbf{p}_\parallel - \mathbf{k}_\parallel}}{[p_z(t) - k_z + i\kappa]^2} + \frac{R\delta_{\mathbf{p}_\parallel - \mathbf{k}_\parallel}}{[p_z(t) + k_z + i\kappa]^2}\right]. \quad (6)$$

Next, we consider the $4f$ core-level band. We model this band with a zero band width in terms of isolated $4f$ atomic wave functions $\psi_c(\mathbf{r})$ localized at the lattice points $\{\mathbf{R}_i\}$

$$\Psi^{\pm}_{\mathbf{k}_i}(\mathbf{r},t) = \sum_i e^{i\mathbf{k}_i^{\pm}\cdot\mathbf{R}_i}\psi_c(\mathbf{r} - \mathbf{R}_i)e^{-i\varepsilon_i t}, \quad (7)$$

where $\varepsilon_i = -32.55$ eV is the $4f$ atomic level binding energy with respect to ε_F, and obtain the DME

$$d^{4f}_{\mathbf{k}_i,\mathbf{p}(t)} = i\delta_{\mathbf{p}_\parallel - \mathbf{k}_\parallel}\frac{d}{dp_z}\{\tilde{\psi}_c[\mathbf{p}(t)]\Delta_{p_z(t),k_z}(\kappa)\}, \quad (8)$$

with $\Delta = \Delta^- - \Delta^+$ and the Fourier transform $\tilde{\psi}_c(\mathbf{p})$ of $\psi_c(\mathbf{r})$. Comparison of the two DMEs (6) and (8) shows that the interlayer structure factor $\Delta^{\pm}$ is canceled by $f^{\pm}_{\mathbf{k}_i,\mathbf{p}(t)}$ for structure-free (completely delocalized) CB electrons in the jellium approximation only, as one might expect. As we show below, this fundamental difference in the localization character of the initial state affects the transport of CB and localized PEs in the presence of an IR-streaking field and is the origin of their observed relative time delay.

Numerical results and comparison with experimental spectra are shown in Fig. 2. We model the $4f$ core state in terms of hydrogenic states $\tilde{\psi}_c(\mathbf{p}) \sim \frac{1}{(p^2 - 2\varepsilon_i)^2}$ because the exact form is not important for our purpose. Our parameters imply peaks in the PE spectra without the IR pulse at $E_c = 55.39$ eV for the core-level electrons and $E_c = 82.43$ eV for the CB electrons.

In order to determine the temporal shift between the CB and $4f$-level band, we calculated the COE of the spectrum $\bar{E}(\tau)$ [23]. In comparison with experimental results (Fig. 3), our model reproduces the measured shift of $\Delta\tau = 110$ as between the COE spectra of these two groups of PEs based on the realistic [24] value $\lambda = 5$ Å. We note that the calculated amplitude of the oscillations in $\bar{E}(\tau)$ [23] in Fig. 3 is about 10 times larger than the experimental amplitude. This is due to a significant background in the COE-averaged experimental data of PEs resulting from above-threshold ionization that is *insensitive* to streaking by the IR pulse [15,31]. Therefore, the temporal shift in energy of the COE of the spectrum is much smaller than that of the photoemission peak alone. Indeed, subtraction of the background in the COE-averaged experimental spectra results in measured streaking amplitudes of 2 and 3.7 eV [31], in better agreement with our calculated amplitudes of 6 and 7 eV for $4f$ and CB PEs, respectively. The remaining discrepancy is subject to further investigations

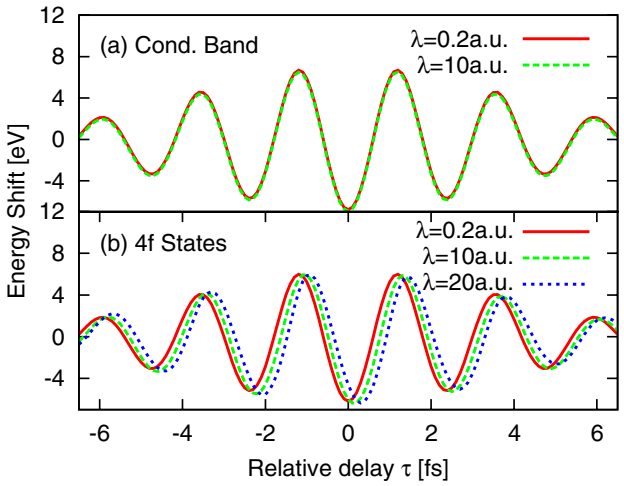

FIG. 4 (color online). Streaked electron spectra for photoemission from (a) CB and (b) $4f$-core levels of a W(110) surface: $\bar{E}$ [23] as a function of the delay between the XUV and IR pulse and the electronic mean free path. Only the streaked electron spectrum from the $4f$-core level is sensitive to the PE mean free path.

[31]. Our calculations indicate that lowering the IR intensities does not change the temporal shift of the streaking oscillations but reduces their amplitudes. In addition, we find that the oscillation amplitudes decrease by increasing the length of the XUV pulse, as expected.

Cavalieri *et al.* [15] pointed out that the slower $4f$ PEs are, on the average, emitted about 1 Å deeper than the faster CB electrons. Our calculations confirm this statement and further specify that there is no dependence of the CB temporal shift on λ [Fig. 4(a)]. In contrast, we find that the temporal shift is most sensitive to the transport properties inside the solid of the $4f$ PEs and increases with λ [Fig. 4(b)]. For very small λ, $\Delta^- \sim 1$ and only core-level electrons from first layer atoms contribute the photocurrent, as for the case of an isolated atom, resulting in no shift compared to that of the CB PEs (Fig. 4). This demonstrates the importance of interlayer interference for the temporal shift of $4f$ core-level PEs and agrees with the intuitive expectation that electrons from deeper layers need more time to reach the surface of the metal and the detector. However, the different temporal behavior of CB and $4f$ PEs as a function of λ also reflects their different electronic and transport properties. We note that weak evidence for different dispersion (chirps) of the CB and $4f$ attosecond PE wave packets is also noticeable in our calculated PE spectra (right column in Fig. 2) by comparing their spectral widths near delays of ≈ -2 and ≈ -0.5 fs at zero energy shift. This difference is due to the broad momentum distribution of $4f$ PEs relative to the narrow momentum spread of individual CB states and is a subject of further investigation. The crucial difference between the DMEs for CB and $4f$ electrons lies in the interlayer structure factor (3) which expresses the temporal phase modulation by the IR field that causes the relative temporal shift.

In conclusion, we have demonstrated that the finite mean free path of photoelectrons and interlayer interference lead to the observed temporal shift between core-level and CB PEs.

We thank Feng He for valuable discussions. This work was supported by the NSF and the Division of Chemical Sciences, Office of Basic Energy Sciences, Office of Energy Research, U.S. DOE.

[1] M. Hentschel *et al.*, Nature (London) **414**, 509 (2001).
[2] P. M. Paul *et al.*, Science **292**, 1689 (2001).
[3] Z. Chang, Phys. Rev. A **70**, 043802 (2004).
[4] G. Sansone *et al.*, Science **314**, 443 (2006).
[5] N. Dudovich *et al.*, Nature Phys. **2**, 781 (2006).
[6] P. B. Corkum and F. Krausz, Nature Phys. **3**, 381 (2007).
[7] E. Goulielmakis *et al.*, Science **320**, 1614 (2008).
[8] M. Drescher *et al.*, Nature (London) **419**, 803 (2002).
[9] R. Kienberger *et al.*, Nature (London) **427**, 817 (2004).
[10] M. Uiberacker *et al.*, Nature (London) **446**, 627 (2007).
[11] P. Johnsson *et al.*, Phys. Rev. Lett. **99**, 233001 (2007).
[12] H. Niikura *et al.*, Nature (London) **421**, 826 (2003).
[13] M. F. Kling *et al.*, Science **312**, 246 (2006).
[14] A. Staudte *et al.*, Phys. Rev. Lett. **98**, 073003 (2007).
[15] A. L. Cavalieri *et al.*, Nature (London) **449**, 1029 (2007).
[16] J. C. Baggesen and L. B. Madsen, Phys. Rev. A **78**, 032903 (2008).
[17] L. Miaja-Avila *et al.*, Phys. Rev. Lett. **101**, 046101 (2008); G. Saathoff *et al.*, Phys. Rev. A **77**, 022903 (2008).
[18] A. Kubo *et al.*, Nano Lett. **5**, 1123 (2005).
[19] M. Sukharev and T. Seideman, Nano Lett. **6**, 715 (2006).
[20] M. I. Stockman *et al.*, Nat. Photon. **1**, 539 (2007).
[21] F. Le *et al.*, Phys. Rev. B **76**, 165410 (2007).
[22] P. B. Corkum, Phys. Rev. Lett. **71**, 1994 (1993).
[23] The COE of the spectrum is defined as $\bar{E}(\tau) = \int_{E_{\min}}^{E_{\max}} dEEP(E,\tau) / \int_{E_{\min}}^{E_{\max}} dEP(E,\tau) - E_c$, where E_c is the spectral peak position without the IR field. We used the same limits as Ref. [15], i.e., $E_{\min} = 47(66)$ and $E_{\max} = 66(110)$ eV for $4f$ (CB) PEs, respectively.
[24] A. Zangwill, *Physics at Surfaces* (Cambridge University Press, Cambridge, England, 1988).
[25] S. Hüfner, *Photoelectron Spectroscopy* (Springer, Berlin, 2003), 3rd ed.
[26] H. M. Milchberg and R. R. Freeman, J. Opt. Soc. Am. B **6**, 1351 (1989).
[27] P. Gibbon, *Short Pulse Laser Interactions with Matter* (Imperial College Press, London, 2005).
[28] M. Kitzler *et al.*, Phys. Rev. Lett. **88**, 173904 (2002).
[29] V. S. Yakovlev, F. Bammer, and A. Scrinzi, J. Mod. Opt. **52**, 395 (2005).
[30] U. Thumm, J. Phys. B **25**, 421 (1992); P. Kürpick *et al.*, Phys. Rev. A **56**, 543 (1997).
[31] Professor Ulrich Heinzmann (private communication).